RESEARCH ARTICLE | NOVEMBER 30 2006

# Proton hydration in aqueous solution: Fourier transform infrared studies of HDO spectra

Maciej Śmiechowski; Janusz Stangret



*J. Chem. Phys.* 125, 204508 (2006)
https://doi.org/10.1063/1.2374891

# Proton hydration in aqueous solution: Fourier transform infrared studies of HDO spectra

Maciej Śmiechowski and Janusz Stangret[a)]
*Department of Physical Chemistry, Chemical Faculty, Gdańsk University of Technology, Narutowicza 11/12, 80-952 Gdańsk, Poland*

(Received 17 July 2006; accepted 4 October 2006; published online 30 November 2006)

This paper attempts to elucidate the number and nature of the hydration spheres around the proton in an aqueous solution. This phenomenon was studied in aqueous solutions of selected acids by means of Fourier transform infrared spectroscopy of semiheavy water (HDO), isotopically diluted in $H_2O$. The quantitative version of difference spectrum procedure was applied for the first time to investigate such systems. It allowed removal of bulk water contribution and separation of the spectra of solute-affected HDO. The obtained spectral data were confronted with *ab initio* calculated structures of small gas-phase and polarizable continuum model (PCM) solvated aqueous clusters, $H^+(H_2O)_n$, $n=2-8$, in order to help in establishing the structural and energetic states of the consecutive hydration spheres of the hydrated proton. This was achieved by comparison of the calculated optimal geometries with the interatomic distances derived from HDO band positions. The structure of proton hydration shells outside the first hydration sphere essentially follows the model structure of other hydrated cations, previously revealed by affected HDO spectra. The first hydration sphere complex in diluted aqueous solutions was identified as an asymmetric variant of the regular Zundel cation [*The Hydrogen Bond: Recent Developments in Theory and Experiments*, edited by P. Schuster, G. Zundel, and C. Sandorfy (North-Holland, Amsterdam, 1976), Vol. II, p. 683], intermediate between the ideal Zundel and Eigen structures [E. Wicke *et al.*, Z. Phys. Chem. Neue Folge **1**, 340 (1954)]. Evidence was found for the existence of strong and short hydrogen bonds, with oxygen-oxygen distance derived from the experimental affected spectra equal 2.435 Å on average and in the PCM calculations about 2.41–2.44 Å. It was also evidenced for the first time that the proton possesses four well-defined hydration spheres, which were characterized in terms of hydrogen bonds' lengths and arrangements. Additionally, an outer hydration layer, shared with the anion, as well as loosely bound water molecules interacting with free electron pairs of the central complex were detected in the affected spectra. © *2006 American Institute of Physics*.
[DOI: 10.1063/1.2374891]



## I. INTRODUCTION

The structure and the properties of the hydrated proton have been studied extensively in decades, due to their importance in biochemistry, atmospheric chemistry, and chemical technology.[1,2] Yet, the actual hydrate structure of proton in diluted aqueous solutions is still unsettled. The two concepts widely used for the description of the phenomenon are the hydrated proton with central $H^+$ and two water molecules, $H_5O_2^+$, and hydrated symmetric hydronium ion, $H_3O^+$, commonly referred to as the "Zundel cation"[3] and the "Eigen cation,"[4] respectively.

The anomalously high ionic mobility of $H^+$ is a nontrivial issue as well, particularly from the point of view of enzymatic catalysis mechanisms. The proton transfer (PT) model of consecutive "proton hops" between neighboring water molecules, referred to as "the Grotthus mechanism," has gradually become the prevailing picture, although with the stipulation that it is the solvation structure that migrates, not the excess proton itself.[5]

The structure of larger protonic water clusters has been thoroughly studied by quantum mechanical (QM) methods.[6–12] The solvation dynamics and PT processes have also received careful attention on the basis of molecular dynamics (MD) or Monte Carlo (MC) studies.[10,13–20]

The geometry optimizations have been usually carried out either at the Hartree-Fock (HF) level or at the MP2 correlated level with fairly large polarized basis sets.[6–8] Density-functional-theory-based calculations have also been reported.[9–12] Both Zundel-type (Z) and Eigen-type (E) cations have been identified in the optimized gas-phase structures.[8–12] With increasing number of water molecules in the cluster, it has become apparent though that the ideal symmetric Z cation fails to be an optimal structure any longer.[10]

Self-consistent reaction field (SCRF) methods, such as the polarizable continuum solvation model (PCM),[21] have found wide application in the study of external solvent influence on the geometry and energetics of the immersed QM-optimized cluster. A coherent approach has been recently reported by Pliego and Riveros in the form of cluster-continuum hydration model.[22] A similar study was reported

a)Electronic mail: stangret@chem.pg.gda.pl



 

earlier for the hydrated proton species.[6] Again, the notion is that including external reaction field favors asymmetric E cations as optimum structures.

Simulation techniques have provided considerable insight into the solvation dynamics of the hydrated proton. Particularly, the equilibrium between the E and Z cations and the reaction pathways connecting both structures might be adequately modeled. In the *ab initio* MD study by Tuckerman *et al.*,[14] the E configuration has been found in ca. 60% of the snapshots, the rest being populated by various intermediate PT states resembling the Z cation. A similar contribution of the Z species (ca. 40%) has been found in the multistate empirical valence bond study by Vuilleumier and Borgis,[18] on the basis of both the geometrical criterion of classification ($R_{OO} < 2.45$ Å) and the occurrence of PT process in a specified amount of time (50 fs). Changing the PT observation time, however, significantly influenced the proportion of both hydrated proton forms and the difficulty of discrimination between two unambiguous structures has been pointed out. This problem has been further addressed in the very recent paper by Asthagiri *et al.*,[13] where the dominant proton complex in an *ab initio* MD run has been identified as a slightly asymmetric Z cation.

Molecular simulations have also allowed computation of vibrational spectrum, usually in the form of vibrational density of states.[10,15–19] The prevailing conclusion has been that the protons in E-type cluster contribute to the 3150–2500 $cm^{-1}$ spectral range,[16,18,19] while the spectral signature of the central proton in the Z cation is an intense absorption in the 1800–1000 $cm^{-1}$ range.[10,16,18,19] An actual comparison of experimental and computed vibrational spectra has also been performed[15] and a satisfactory agreement has been concluded, both for $H^+/H_2O$ and $D^+/D_2O$ cases. In other studies, the isotope substitution effect on the hydrated proton has seemed to be minor from the energetic point of view.[17,18]

Vibrational spectroscopy is a valuable tool for the investigation of solute hydration.[23,24] Both Raman[25–27] and IR (Refs. 3, 15, and 28–34) spectroscopies have been hitherto used in revealing the proton hydration. The concept of so-called "extremely polarizable" hydrogen bonds, acting as proton transfer pathways, was inferred on the basis of some measurements.[3,30,31,35] The "infrared continua," however, a prominent feature of the IR spectra,[15,28–32] have been virtually absent in the Raman measurements.[25–27] Consequently, the exact nature of the hydrated proton from the vibrational spectroscopy point of view has been an arguable issue.[3,36] More recent papers tend to underline the dynamic equilibrium between the E and Z cations,[15] a conclusion supported also by gas-phase IR spectroscopy of size-selected cluster ions.[37]

Spectra of isotopically diluted HDO in $H_2O$ are free from most of experimental and interpretative problems connected with $H_2O$ spectra.[38–40] The decoupled OD water vibrations appear to be the most sensitive and ideally suited probe of ionic hydration. To extract information about the interactions inside the hydration sphere, the contribution of bulk water should be eliminated from the solution spectrum to obtain the solute-affected water spectrum. The corresponding method of spectral data analysis was proposed by Kristiansson *et al.*[41,42] The quantitative version of this method was formulated later by these authors and independently in our laboratory.[43,44] Since then, a large number of solutes have been studied this way and a recent review summarizes available experimental data.[45] The most important factor in the interpretation of HDO spectra is the band position. The empirical Badger-Bauer rule[46] states that the position of the water stretching band changes proportionally with the energy of a hydrogen bond. Thus, the solute-affected HDO spectra give valuable information about the energetic states of perturbed water. Particularly, they allow the discrimination between ionic "structure makers" and "structure breakers," in the sense of increasing or decreasing average hydrogen bond energy between the first hydration sphere and the bulk phase. Further hydration spheres can also be quantitatively characterized.[45,47]

The interpretation of HDO spectral data for cations was further strengthened with the introduction of generalized cation hydration theory, formulated in our group.[45] It was experimentally verified, on the basis of numerous solutes, that cation-affected HDO band position did not change in a continuous manner. Instead, the band positions tended to group in broadly defined levels, found at 2200, 2420, and 2533 $cm^{-1}$ (cf. Fig. 5 of Ref. 45). The spectral data used to formulate the theory encompassed mono-, di-, and trivalent metal cations, as well as representative hydrophobic cations, such as $Bu_4N^+$ or $Ph_4P^+$. The relevance of this model to the case of the hydrated proton is discussed in Sec. IV A.

HDO vibrational spectra can also provide basic structural characteristics of the solute-affected water, as the OD band position can be correlated with interatomic oxygen-oxygen distance. Several correlations linking $R_{OO}$ with $\nu_{OD}$ have been published[48,49] and successfully used in the studies on ion hydration.[42,47,50]

Although the isotopic dilution method has proven its usefulness, it has only once been applied in the investigation of proton hydration.[34] Quite different interpretation used by these authors justifies further studies with this technique.

In this work, we correlate the picture of hydrated proton emerging from Fourier transform infrared (FTIR) measurements of OD band of isotopically diluted HDO molecules with the *ab initio* calculated structures of small aqueous clusters, $H^+(H_2O)_n$, trying to establish the structural and energetic states of the consecutive hydration spheres of the hydrated proton. This has been achieved with assistance of comparison of the calculated optimal geometries with the interatomic distances derived from the HDO band position using the above-mentioned correlation. It is common knowledge that analytically calculated vibrational frequencies only qualitatively correlate with experimental results for liquid phases, even when scaled or otherwise corrected for anharmonicity. Consequently, they have been rejected by us in favor of the indirect comparison.

## II. EXPERIMENT

### A. Chemicals and solutions

The following aqueous solutions of acids were obtained from respectable manufacturers and used as supplied: HCl (POCh S.A., analytical amount), $HClO_4$ (70% aqueous, A.C.S. reagent, Aldrich), and $HPF_6$ (65% aqueous, Lancaster). $D_2O$ used in the preparation of solutions came from two sources: Institute of Nuclear Investigation, Poland (99.84% isotopic purity) and Aldrich (99.96% isotopic purity).

Stock solutions were prepared by mixing weighed amounts of respective aqueous acids with redistilled water. The molalities of stock solutions were checked by conductometric titration with a standard base and were 0.894 mol $kg^{-1}$ for HCl, 1.067 mol $kg^{-1}$ for $HClO_4$, and 0.803 mol $kg^{-1}$ for $HPF_6$. The series of solutions, spanning the molality range from ca. 0.2 mol $kg^{-1}$ to stock concentration, were prepared by mixing weighed amounts of the respective stock solution with redistilled water. Sample solutions were made by adding 4% (by weight) of $D_2O$ relative to $H_2O$ and reference solutions by adding the same molar amounts of $H_2O$. All manipulations involving $HPF_6$ were performed in polypropylene vessels.

Densities of HCl and $HClO_4$ solutions were measured on an Anton Paar DMA 5000 density meter at (25.000±0.001) °C. Densities of $HPF_6$ solutions were measured on a UniLab MG-2 density meter at 10.0±0.1, 15.0±0.1, 25.0±0.1, 35.0±0.1, and (45.0±0.1) °C.

### B. FTIR measurements

FTIR spectra were recorded on an IFS 66 Bruker spectrometer. 256 scans were made with a selected resolution of 4 $cm^{-1}$. A cell with $CaF_2$ windows was employed. The path length was 0.0298 mm, as determined interferometrically. The temperature was kept at (25.0±0.1) °C by circulating thermostated water through mounting plates of the cell. The temperature was monitored by a thermocouple inside the cell. For the temperature series of $HPF_6$, the measurement temperatures were 10.0±0.2, 15.0±0.2, 25.0±0.2, 35.0±0.2, and (45.0±0.2) °C.

### C. Data analysis

The spectra were handled and analyzed by the commercial personal computer (PC) programs GRAMS/32 (Galactic Industries Corporation, Salem, MA) and RAZOR (Spectrum Square Associates, Ithaca, NY) run under GRAMS/32. Two dimensional (2D) correlation analysis was performed with the SPECTRACORR software (Thermo Electron Corporation, Madison, WI).

The measured HDO spectra were transformed to molar absorption coefficient scale and interpolated from their dependence on molality. Linear or quadratic relationships adequately described the absorption change with molality, $R^2 > 0.999$ at any given wave number. The derivative in the infinite dilution approximation, $(\partial\varepsilon/\partial m)_{m=0}$, was then calculated from the interpolated spectra. For the temperature series of $HPF_6$, the spectra were first interpolated from their temperature dependence (described properly by a quadratic relationship, $R^2 > 0.99$) and then, at each of the given temperature points, subjected to further treatment as above.

The difference spectrum method was used to analyze the influence of solute on the solvent structure. It is based on the assumption that water in the solution may be divided into additive contributions of solute-affected ($a$) and bulk ($b$) water. The "affected" HDO spectra, $\varepsilon_a$, were calculated from the derivative spectrum and the bulk HDO spectrum, $\varepsilon_b$, according to

$$\varepsilon_a = \frac{1}{NM}\left(\frac{\partial\varepsilon}{\partial m}\right)_{m=0} + \varepsilon_b. \quad (1)$$

In (1), $M$ is the mean molecular mass of the solvent ($H_2O$+4% $D_2O$) and $N$ is the assumed "affected number," or number of moles of solvent affected by 1 mol of solute. The procedure of finding the proper value of $N$ by systematic analysis and band fitting of affected spectra has been previously described in detail.[50] $N$ is an empirical parameter and should not be, in principle, identified as hydration number. In many cases though, when the cation- and anion-affected bands are sufficiently separated, it is close to hydration number derived from direct methods.

In this work, before calculating the affected spectra, the region 1900–1500 $cm^{-1}$ was manually smoothed in both the derivative spectrum and the bulk HDO spectrum, to remove the noise from highly absorbing $H_2O$ deformation band. This procedure has not been applied before in our laboratory, since the affected HDO spectra have never been redshifted beyond 2000 $cm^{-1}$.[45,47,50,51]

## III. COMPUTATIONAL DETAILS

Small aqueous clusters, $H^+(H_2O)_n$, $n=2-8$, were used as model systems in the calculations, with maximal $n$ dependent on the basis set and level of theory. *Ab initio* calculations were performed with the use of standard Pople basis set 6-311++G($d$,$p$).[52] For comparison purposes, a much more exhaustive basis set from the correlation-consistent family, aug-cc-pVTZ,[53,54] was used for some systems. Both basis sets are of the *triple-zeta* type, i.e., with triple split valence orbitals, and are augmented with polarization and diffuse functions on both heavy atoms and hydrogens, although the aug-cc-pVTZ basis is more heavily polarized than the 6-311++G($d$,$p$).

Post-HF treatment of electron correlation effects was done in the framework of second-order Møller-Plesset perturbation theory,[55] with the frozen-core approximation for oxygen inner-core (1$s$) electrons.

Density functional theory calculations used the B3LYP combination functional,[56] composed of B88 exchange functional[57] and LYP correlation functional,[58] and containing a portion of Hartree-Fock exchange. Numerical integrations used an *UltraFine* grid, which is a pruned (99,590) grid, consisting of 99 shells per atom and 590 points per shell.

Basis set superposition error (BSSE) effects were neglected in the calculations, as the commonly used counter-

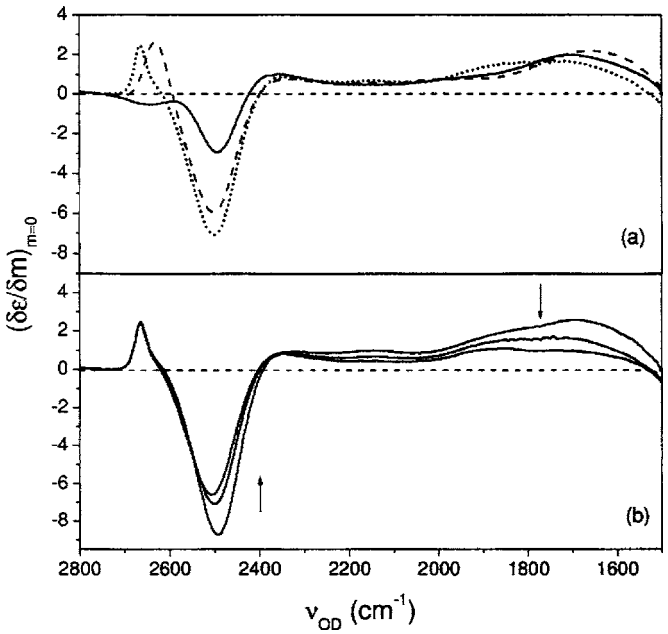


FIG. 1. (a) Derivatives $(\partial\varepsilon/\partial m)_{m=0}$ in the OD stretching region for aqueous solutions of HCl (solid line), $HClO_4$ (dashed line), and $HPF_6$ (dotted line) for linear relationship of $\varepsilon$ vs $m$. (b) Temperature dependence of the derivative for $HPF_6$ aqueous solutions in the range 10–45 °C (arrows indicate increasing temperature).

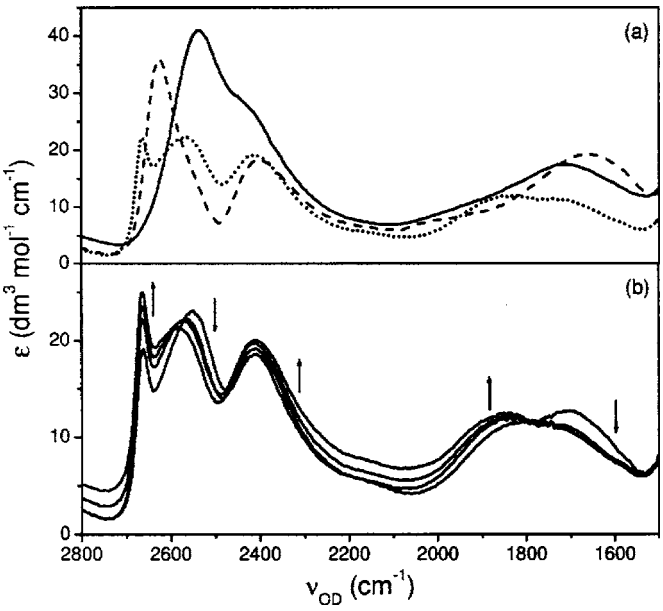


FIG. 2. (a) Affected HDO spectra in the OD stretching region for HCl (solid line), $HClO_4$ (dashed line), and $HPF_6$ (dotted line) aqueous solutions. (b) Temperature dependence of the $HPF_6$-affected HDO spectrum in the range 10–45 °C (arrows indicate increasing temperature).

poise algorithm tends to overestimate their contribution, particularly for electron correlation methods. This fact has been confirmed for $H^+(H_2O)_n$ clusters.[7]

Initial structures of all studied systems belonged to the $C_1$ symmetry group and no symmetry constraints were imposed during geometry optimization. Berny algorithm[59] with *Tight* convergence criteria was used for optimizations. The GDIIS method[60] (geometry optimization using direct inversion in the iterative subspace) was used for most of the systems to speed up convergence. Vibrational analysis was performed on optimized structures to check for true minima and calculate zero-point energy (ZPE) corrections.

Gas-phase cluster structures were subsequently used as starting points for further geometry optimization in the SCRF approach. The standard polarizable continuum solvation model[21] was used, with united atom topological model applied on atomic radii optimized for the HF/6-31G($d$) level of theory (UAHF), as implemented in the GAUSSIAN 03 system.[61] Vibrational analysis for PCM optimized structures was performed in the numeric approximation.

All calculations were performed with the GAUSSIAN 03 system.[61] HYPERCHEM 6.0 (Hypercube, Inc., Gainesville, FL) and GAUSSVIEW 3.0 (Gaussian, Inc., Pittsburgh, PA) served as front-end interfaces and visualization tools.

## IV. RESULTS AND DISCUSSION

### A. Affected HDO spectra

The derivatives $(\partial\varepsilon/\partial m)_{m=0}$ for the three studied acids at 298 K are shown in Fig. 1(a). The temperature dependence of the derivative for $HPF_6$ is illustrated in Fig. 1(b). The most important difference between the derivatives for acid solutions shown here and those for other solutes previously studied in our laboratory[45,47,50,51] is the extension of the derivative spectrum beyond 2000 $cm^{-1}$.

The affected spectra, calculated for the three studied acids at 298 K from Eq. (1), are shown in Fig. 2(a). The following adjusted $N$ values were found: $N=7.0$ ($HClO_4$), $N=8.0$ (HCl), and $N=9.3$ ($HPF_6$). The evolution of affected spectra with temperature for the $HPF_6$ series is depicted in Fig. 2(b). Apart from the lowest (10 °C, $N=11.0$) and the highest (45 °C, $N=10.0$) temperatures studied, $N$ remained constant throughout the whole series ($N=9.3$–$9.4$). The $N$ values observed here compare well with our previous studies of simple electrolytes, where we have found $N=7.0$ for $NaClO_4$,[51] $N=8.1$ for $Bu_4NCl$,[50] and $N=9.8$ for $KPF_6$.[47] It can be inferred from these numbers that proton affected about five to six water molecules.

As before, the obvious distinguishing feature of the proton-affected HDO spectra is their extension well below the 2000 $cm^{-1}$ boundary. Unlike in the infrared spectra of $H_2O$ acidic solutions,[15,28–32] however, the broad band observed for HDO cannot be adequately described as a "continuum." Instead, it shows a distinctive structure that could be adequately resolved into simple component bands. The decomposition of the affected HDO spectra into components is depicted in Fig. 3 for the three studied acids at 298 K. The absence of continuum in HDO spectra is a consequence of isotopic decoupling of vibrational modes of the system.

The multicomponent affected water band contains contribution from HDO affected by anionic component of the electrolyte. The respective bands are located at 2631 $cm^{-1}$ for $ClO_4^-$ in $HClO_4$,[45] at 2666 $cm^{-1}$ for $PF_6^-$ in $HPF_6$,[45,47] and at 2544 $cm^{-1}$ for $Cl^-$ in HCl.[45,50] The latter is slightly different than the previously reported band position for $Cl^-$, but this should be attributed to a superposition with the component band of the proton-affected water, as discussed later.

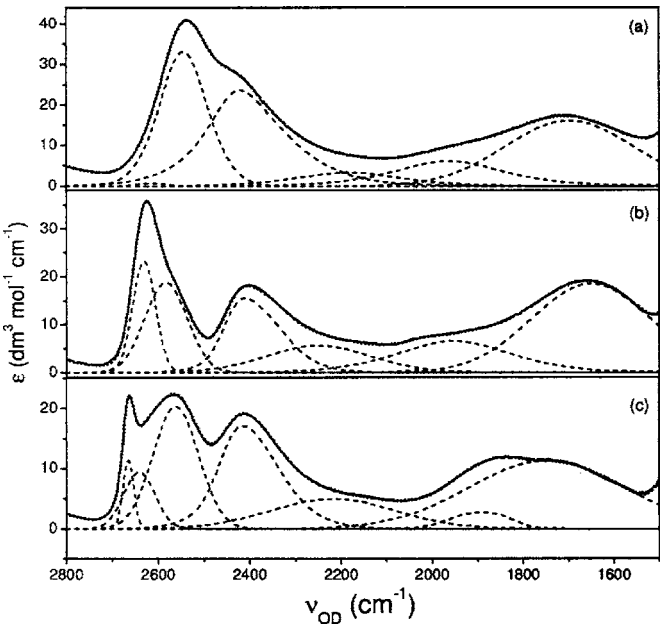


FIG. 3. Decomposition of the affected HDO spectra into component bands for (a) HCl, (b) $HClO_4$, and (c) $HPF_6$ at 298 K. Solid line: original affected spectrum, dashed lines: component bands, and dotted line: sum of the component bands.

The $PF_6^-$ anion used in this work has the tremendous advantage of being one of the strongest structure-breaking ions in water.[45] Thus, the position of $PF_6^-$-affected HDO band is very strongly blueshifted with respect to bulk HDO. Although other anions, notably $BF_4^-$ or $ClO_4^-$, also exert major structure-breaking effect,[45] the application of hexafluorophosphates provides deeper insight into cation-affected HDO band, as the anionic component can be adequately separated from the affected HDO spectrum. This approach previously allowed unambiguous resolving of the "cation+anion-affected" HDO band, which is typically obscured by the anion-affected component.[47] Consequently, we have selected $HPF_6$ as a "model" acid for this work, as the cation-affected HDO bands are best separated in this case and the temperature-dependent studies could potentially reveal more important information.

The parameters of the affected HDO bands that can be attributed to the hydrated proton are listed in Table I for the three studied acids at 298 K. The temperature dependencies of the chosen band parameters for $HPF_6$ are illustrated in Fig. 4.

The outermost hydration sphere of the proton complex, detectable with our method of analysis, manifests itself by a single band in the HCl and $HPF_6$ affected HDO spectra. The position of this band depended approximately linearly on the kind of counteranion.[47] The values found in the present work are 2613 $cm^{-1}$ for HCl and 2636±5 $cm^{-1}$ (value interpolated from temperature dependence) for $HPF_6$ at 298 K, in satisfactory agreement with the published correlation and the data available for other hexafluorophosphates.[47] For $HClO_4$, the discussed band could not be resolved. Based on the correlation, we would expect it to appear at ca. 2630 $cm^{-1}$, where the affected spectrum is dominated by the prominent anion-affected HDO band.

A brief inspection of Table I reveals that other proton-affected HDO component bands also depended on the kind of anion. This dependence was notable especially for the band at ca. 1700 $cm^{-1}$, but other bands were more or less shifted by the anion as well. The possible influence of the anion on the hydrated proton complex will be further investigated below.

The band positions quoted in Table I can be discussed in view of the cation hydration theory, derived on the basis of HDO vibrational spectra measurements, previously formulated in our group[45] The observation that HDO band posi-

TABLE I. Parameters of component bands attributed to the hydrated proton from the decomposition of the HDO spectra affected by HCl, $HClO_4$, and $HPF_6$ at 298 K. The band at ca. 1950 $cm^{-1}$ is excluded as not originating from the stretching HDO vibration.

| | HCl | | $HClO_4$ | | $HPF_6$[b] | |
|---|---|---|---|---|---|---|
| Assignment[d] | $\nu_{OD}^{o}$[c] ($cm^{-1}$) | FWHH[d] ($cm^{-1}$) | $\nu_{OD}^{o}$[c] ($cm^{-1}$) | FWHH[d] ($cm^{-1}$) | $\nu_{OD}^{o}$[c] ($cm^{-1}$) | FWHH[d] ($cm^{-1}$) |
| Fifth sphere (shared with anion) | 2613 | 81 | …[e] | …[e] | 2636 | 86 |
| "Donor pair" | 2544[f] | 124 | 2583 | 111 | 2561 | 105 |
| Fourth sphere[g] | … | … | … | … | ~2530 | … |
| Third sphere | 2421[h] | 196 | 2409[h] | 145 | 2413[h] | 159 |
| Second sphere | 2183 | 275 | 2249 | 273 | 2202 | 320 |
| First sphere | 1697 | 331 | 1651 | 310 | 1747 | 404 |

[a]Hydration spheres numbered consecutively from the central proton, "donor pair" refers to the water molecule coordinated to the free electron pair of oxygen in the central proton complex.
[b]Values interpolated from the temperature dependence.
[c]Band position at maximum.
[d]Full width at half-height.
[e]Respective band could not be resolved in the decomposed affected spectrum.
[f]Superposition with the anion-affected HDO band (see text for details).
[g]Band detectable only in the 2D-IR correlation spectra from the temperature dependence of the affected spectrum for $HPF_6$.
[h]Composite band.

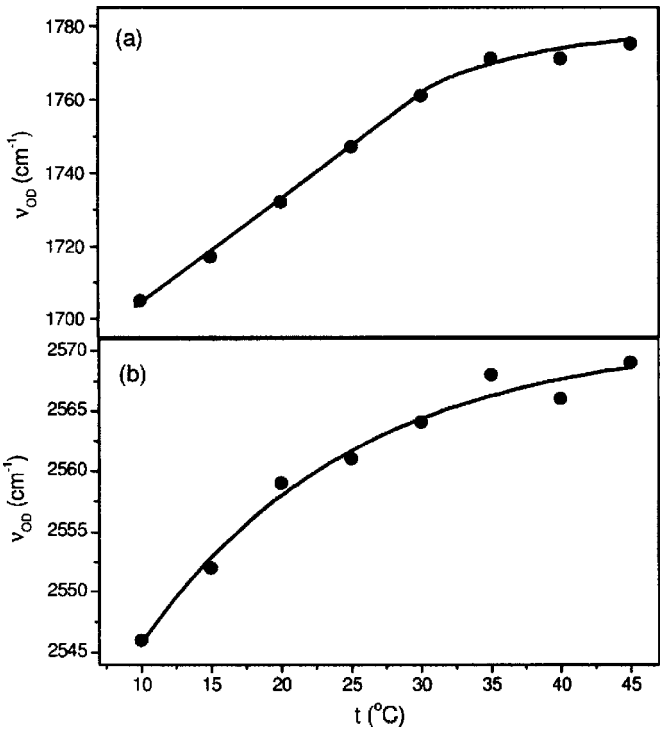


FIG. 4. Temperature dependence of selected component bands' parameters for the $HPF_6$-affected HDO spectrum: (a) band position at maximum of the ca. 1750 cm$^{-1}$ component; (b) band position at maximum of the ca. 2560 cm$^{-1}$ component.

tions for cations do not change in a continuous manner, but rather group into broadly defined levels instead, is invaluable in the interpretation of spectral data. The results found here for the hydrated proton are partially in accordance with that model. The particular cases can be described in detail as follows. The band at 2409–2421 cm$^{-1}$ belongs to the level formed mainly by divalent transition metal cations ($\nu_{OD}$ =2420±20 cm$^{-1}$) and can be qualitatively described as "ice-like" water (in terms of HDO band position, which is 2420 cm$^{-1}$ in deuterium-doped ice).[62] The band at 2183–2249 cm$^{-1}$ is notably close to the level containing trivalent metal cations with a high polarizing power, such as $Rh^{3+}$, $Cr^{3+}$, or $Al^{3+}$ ($\nu_{OD}$=2200±20 cm$^{-1}$) and is indicative of very strong hydrogen bonds. On the basis of the previously observed regularities in the occurrence of the levels,[45] an as yet undetected level might be expected at ca. 1705–1815 cm$^{-1}$, with hydrated $H^+$ as the only representative. The respective band was actually found in the measured spectra at 1651–1747 cm$^{-1}$. Thus, although the hydrated proton is fundamentally different from all other cations used to construct the original model, the positions of the component bands in its affected HDO spectrum do follow the general pattern outlined in the model and even expand it by adding a new band position level at low $\nu_{OD}$.

The component band located at ca. 1963–1891 cm$^{-1}$ falls outside the scope of the discussed cation hydration model. It should, however, be noted that the bulk HDO spectrum shows a weak band in this area as well (at about 1850 cm$^{-1}$). Its counterpart in the $H_2O$ infrared spectrum, weak band at approximately 2100 cm$^{-1}$, has been commonly interpreted as a combination of bending and libration

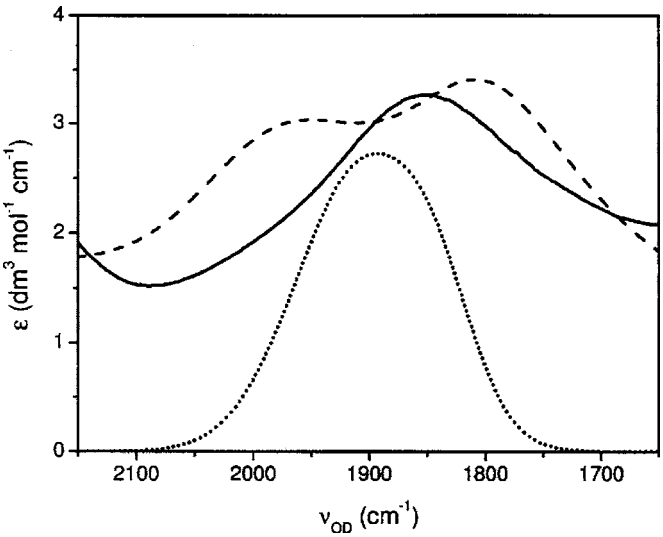


FIG. 5. The $\nu_2+\nu_L$ combination of bending and libration tones in the bulk HDO spectrum (4% w/w HDO in $H_2O$) (solid line), in the spectrum of HDO affected by $KPF_6$ (Ref. 47) (dashed line) and as a component band in the $HPF_6$-affected HDO spectrum (dotted line).

modes.[63] As such, it has no connection whatsoever with the stretching modes, but still can be detected in the difference spectra, being influenced by the solute as all other bands in the vibrational spectrum. On the basis of HDO spectra of numerous electrolyte solutions, we are quite certain that the band in question actually remains in the difference spectrum, usually slightly modified (cf. Fig. 5). The evidence thus strongly suggests that a residuum of HDO combination band should be anticipated at ca. 1900–1850 cm$^{-1}$ rather than a genuine component of the stretching vibration band.

The complexity of the vibrational spectrum of HDO affected by the hydrated proton encouraged us to proceed with the temperature studies, in order to detect possible equilibria.

### B. Temperature dependence of the affected spectra

As mentioned before, the temperature dependencies of selected results for the $HPF_6$ series are illustrated in Figs. 1, 2, and 4. It is readily seen from Fig. 2 that the spectral components underwent position shifts and intensity changes with temperature, reflecting the changes in the relative proportions of water in different chemical surroundings. All hydrated proton bands were blueshifted, except the one at 2413 cm$^{-1}$, which position remained constant within ±4 cm$^{-1}$. The integrated intensity of this band, and the one at 1747 cm$^{-1}$, increased, while other bands displayed decreased intensity with temperature.

To improve the detection of spectral changes within temperature series, we calculated generalized synchronous and asynchronous 2D correlation spectra from the HDO affected spectra. The generalized algorithm proposed by Noda,[64] implemented in the SPECTRACORR software, was applied. The respective correlation maps are presented in Fig. 6. The maps allowed us to link spectral regions, which interdependence passed undetected in the decomposition of affected spectra. Notable positive synchronous correlation peaks (in the order of decreasing correlation coefficient) were located at 2434–2530, 1692–2530, and 2050–2672 cm$^{-1}$. Negative

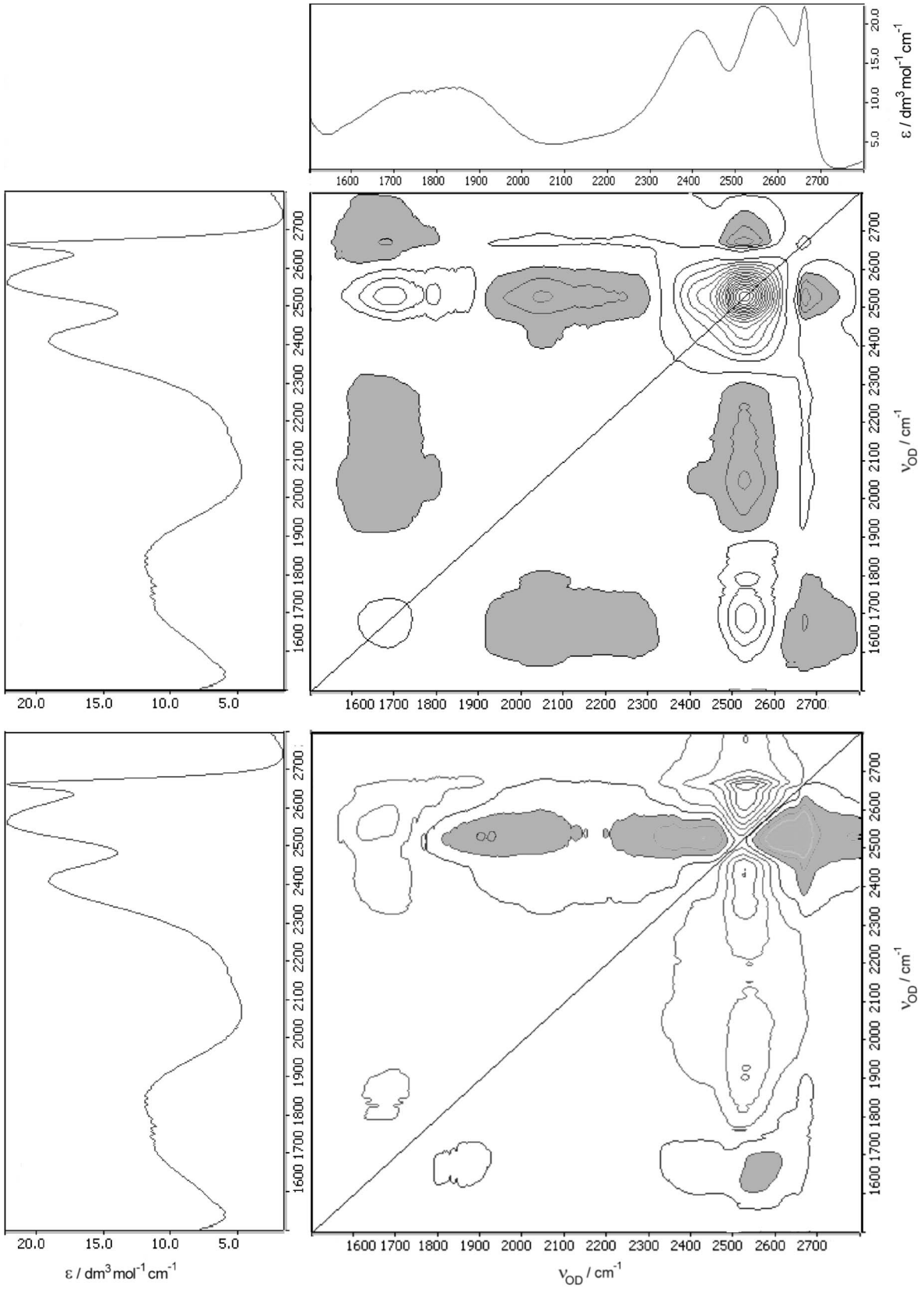


FIG. 6. Synchronous (a) and asynchronous (b) generalized 2D correlation spectra prepared from the temperature series of $HPF_6$-affected HDO spectra. Significant negative correlation indicated by shading. The reference spectrum is the affected spectrum at 298 K.

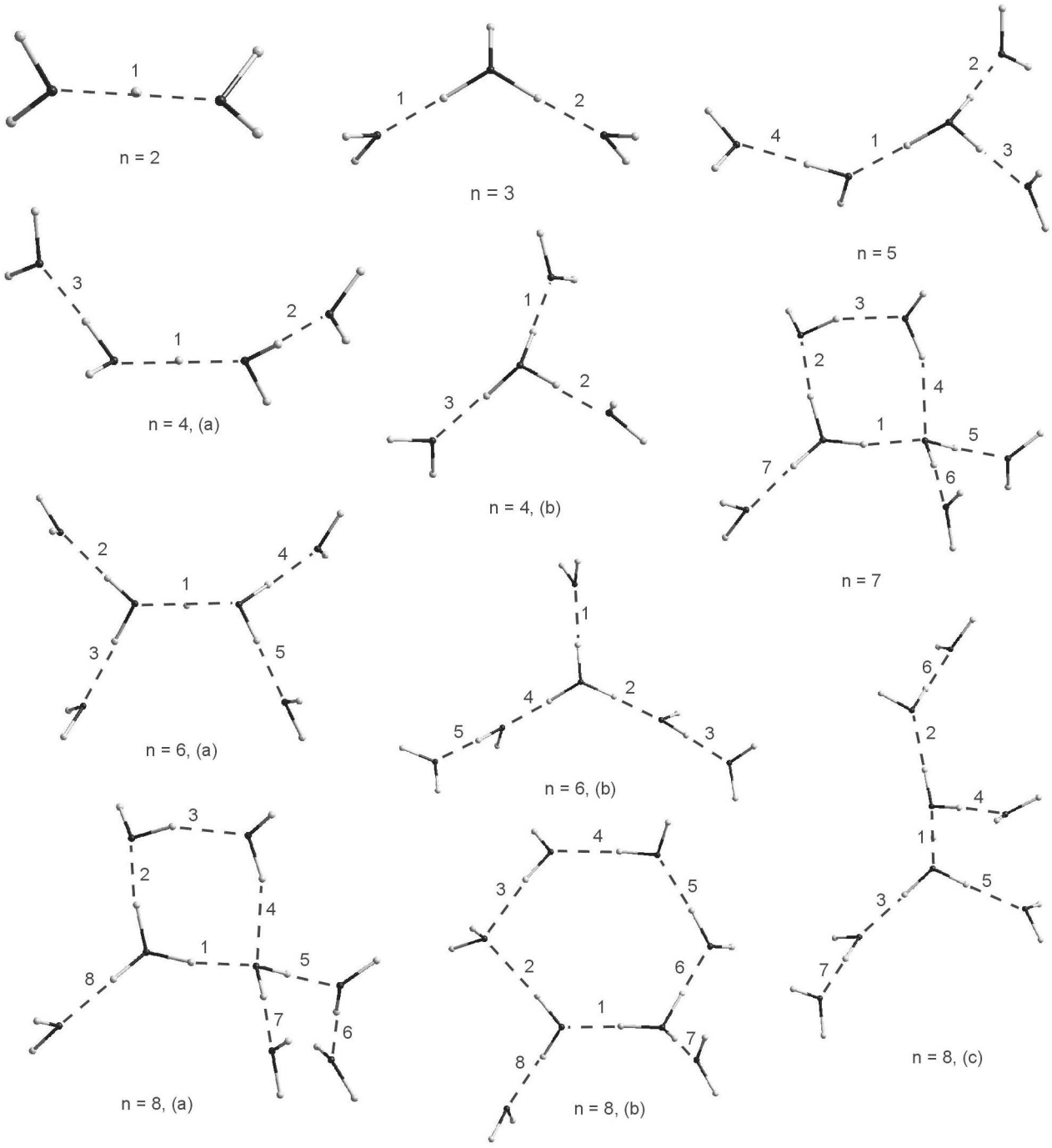


FIG. 7. Hydrated proton clusters, $H^+(H_2O)_n$, studied in this work, in their B3LYP/6-311++G($d$,$p$) gas-phase optimized geometries. Darker spheres denote oxygens, lighter spheres hydrogens. The numbers over hydrogen bonds refer to columns in Tables II and IV.

synchronous cross peaks were found at 2062–2530, 2530–2670, 1670–2672, and 1670–2050 $cm^{-1}$. Asynchronous correlation peaks appeared at 2533–2666, 2440–2532, 1908–2532, 1659–2562, 2200–2530, and 1670–2430 $cm^{-1}$.

Two important and previously unresolved peaks were detected in the correlation maps at ca. 2050 and 2530 $cm^{-1}$. Respective bands disappeared in the decomposition of affected spectra, unless their positions had been fixed. The 2530 $cm^{-1}$ band is in accordance with the quoted cation hydration model[45] and the 2050 $cm^{-1}$ band's significance in the proposed proton hydration model will be discussed below.

### C. *Ab initio* results

Figure 7 shows the structures studied in this work in their optimized gas-phase geometries. The only geometric parameter relevant in the discussion of the HDO spectra is the interatomic oxygen-oxygen distance, $R_{OO}$. The geometry of the studied clusters was fairly conserved between various methods and basis sets of similar complexity. An elongation of interatomic distances in B3LYP versus MP2 level of theory and in aug-cc-pVTZ versus 6-311++G($d$,$p$) basis set might be generally observed. The difference in $R_{OO}$, how-

TABLE II. Optimized intermolecular oxygen-oxygen distances in the studied $H^+(H_2O)_n$ gas-phase clusters at B3LYP/6-311++G($d$,$p$) level of theory. .

| | $R_{OO}$ (Å)[a] | | | | | | | |
|---|---|---|---|---|---|---|---|---|
| $n$ | 1 | 2 | 3 | 4 | 5 | 6 | 7 | 8 |
| 2[b] | 2.394 | | | | | | | |
| 3[c] | 2.492 | 2.492 | | | | | | |
| 4 (a)[d] | 2.391 | 2.596 | 2.581 | | | | | |
| 4 (b)[e,f] | 2.560 | 2.560 | 2.560 | | | | | |
| 5 | 2.475 | 2.596 | 2.595 | 2.681 | | | | |
| 6 (a)[b,d] | 2.393 | 2.679 | 2.674 | 2.679 | 2.674 | | | |
| 6 (b)[e] | 2.621 | 2.510 | 2.704 | 2.513 | 2.703 | | | |
| 7 | 2.552 | 2.492 | 2.665 | 2.886 | 2.733 | 2.745 | 2.624 | |
| 8 (a) | 2.520 | 2.507 | 2.668 | 2.869 | 2.654 | 2.768 | 2.756 | 2.636 |
| 8 (b) | 2.514 | 2.918 | 2.918 | 2.730 | 2.619 | 2.479 | 2.643 | 2.752 |
| 8 (c) | 2.395 | 2.614 | 2.613 | 2.711 | 2.709 | 2.761 | 2.760 | |

[a]The numbers refer to respective labels in Fig. 7.
[b]$C_2$ symmetry group.
[c]$C_s$ symmetry group.
[d]Zundel-type structure.
[e]Eigen-type structure.
[f]$C_3/C_{3v}$ symmetry group.

ever, did not exceed 0.067 Å in the extreme case for gas-phase clusters. On the basis of this important finding, only the values at B3LYP/6-311++G($d$,$p$) level of theory are shown in Tables II–V, in order to simplify the presentation of results. We do, however, mention other levels of theory in the following discussion, when some differences from the presented results occur.

The calculated gas-phase $R_{OO}$ values are shown in Table II. Some structures spontaneously converged towards higher symmetry—this fact is indicated in the table. The B3LYP geometries were similar to the $H^+(H_2O)_{2-6}$ structures computed at the P86/DZVP level by Wei and Salahub,[9] but our interatomic distances were systematically shorter by about 0.05 Å. Larger hydrated proton clusters, $H^+(H_2O)_{7-8}$, were also previously studied by these authors, but the energetic minima obtained in the present work were even qualitatively different from the published ones,[10] thus no direct geometry comparison was possible. This fact is understandable, if we take into account that potential energy surface for so large aggregates is usually very complicated and contains multiple minima.[10,11] For $n=4$ and $n=6$ cases we found two minima, corresponding to both E-type and Z-type cations. The starting point for $H^+(H_2O)_7$ was the Z-type $H^+(H_2O)_6$ geometry with an additional water molecule that formed a hydrogen bond with the free electron pair of one of the oxygens in the central $H_5O_2^+$ structure. The starting points for $H^+(H_2O)_8$ were (a) converged $H^+(H_2O)_7$ structure with an additional water molecule in the second hydration sphere; (b) two water molecules added to Z-type $H^+(H_2O)_6$ geometry as described above for $H^+(H_2O)_7$; (c) Z-type $H^+(H_2O)_6$ geometry with two water molecules added approximately symmetrically in the second hydration sphere of the central $H_5O_2^+$ structure.

TABLE III. Electronic energies and zero-point energies of the studied $H^+(H_2O)_n$ gas-phase clusters at B3LYP/6-311++G($d$,$p$) level of theory.

| $n$ | $E_0$ (hartree) | ZPE[a] (hartree) |
|---|---|---|
| $H_2O$ | −76.458 532 | 0.020 921 |
| 1 | −76.731 236 | 0.033 700 |
| 2 | −153.248 220 | 0.055 909 |
| 3 | −229.746 213 | 0.081 363 |
| 4 (a)[b] | −306.232 103 | 0.103 979 |
| 4 (b)[c] | −306.237 337 | 0.105 753 |
| 5 | −382.718 907 | 0.129 577 |
| 6 (a)[b] | −459.197 818 | 0.151 793 |
| 6 (b)[c] | −459.198 805 | 0.153 793 |
| 7 | −535.675 429 | 0.179 707 |
| 8 (a) | −612.151 787 | 0.203 798 |
| 8 (b) | −612.153 193 | 0.203 883 |
| 8 (c) | −612.151 227 | 0.199 889 |

[a]Scaled zero-point energy (see text for scale factors).
[b]Zundel-type structure.
[c]Eigen-type structure.

The relative stability of the studied systems differed slightly with respect to basis set (cf. Table III). The importance of including zero-point corrections is best seen for two forms of $H^+(H_2O)_6$ clusters. Taking the B3LYP/6-311++G($d$,$p$) energies as an example, while electronic energy of the E form was ca. 2.6 kJ mol$^{-1}$ lower than the Z form, the reverse was true for the ZPE corrected values—here Z form was 2.7 kJ mol$^{-1}$ more stable than the E form. Appropriate scaling of harmonic zero-point energy is of course a problematic issue, especially when no adequate scale factors are available for a particular method and/or basis set. In this work we used the scale factor recommended for the B3LYP/6-31G(2$df$,2$p$) basis set, equal to 0.983,[65] in the scaling of all B3LYP energies and the scale factors proposed for MP2/6-311G($d$,$p$) (0.9748) (Ref. 66) and MP2/cc-pVDZ (0.979) (Ref. 67) in the scaling of 6-311++G($d$,$p$) and aug-cc-pVTZ MP2 energies, respectively. A remarkable change in cluster stability was observed on going from $n=4$ to $n=6$. While for $n=4$, the Z form is less favorable than

TABLE IV. Optimized intermolecular oxygen-oxygen distances in the studied $H^+(H_2O)_n$ PCM-solvated clusters at B3LYP/6-311++G($d$,$p$) level of theory.

| | $R_{OO}$ (Å)[a] | | | | | | | |
|---|---|---|---|---|---|---|---|---|
| $n$ | 1 | 2 | 3 | 4 | 5 | 6 | 7 | 8 |
| 2 | 2.401 | | | | | | | |
| 3 | 2.493 | 2.493 | | | | | | |
| 4 (a)[b] | 2.420 | 2.628 | 2.533 | | | | | |
| 4 (b)[c] | 2.547 | 2.547 | 2.547 | | | | | |
| 5 | 2.500 | 2.560 | 2.558 | 2.683 | | | | |
| 6 (a)[b] | 2.439 | 2.590 | 2.591 | 2.702 | 2.704 | | | |
| 6 (b)[c] | 2.572 | 2.516 | 2.692 | 2.517 | 2.691 | | | |
| 7 | 2.541 | 2.527 | 2.699 | 2.853 | 2.707 | 2.706 | 2.568 | |
| 8 (b) | 2.486 | 2.798 | 2.842 | 2.730 | 2.659 | 2.520 | 2.588 | 2.715 |

[a]The numbers refer to respective labels in Fig. 7.
[b]Zundel-type structure.
[c]Eigen-type structure.

the E form (by about 10 kJ mol$^{-1}$), for $n$=6, on the contrary, the Z form was more stable, provided zero-point correction was included. In both cases, isomer energies calculated at the MP2 level differed more than at the B3LYP level. For the largest studied clusters ($n$=8), changing the level of theory dramatically altered the relative stability of the three isomers. In MP2 calculations, the (b) form was identified as the most stable, while in B3LYP calculations the same could be inferred of the (c) form.

The inclusion of external solvent field via PCM approach resulted in remarkable changes of most interatomic distances (Table IV). The most striking difference occurred for the Z-type cations for $n$=2, 4, and 6. The central very short hydrogen bond underwent elongation by 0.006–0.055 Å, with simultaneous movement of the central proton from the center of the bond towards one of the oxygens. The final result was a transition from a symmetric Zundel cation to an asymmetric Z/E intermediate; this structural feature was best seen for the $H^+(H_2O)_6$ clusters. Nevertheless, still two isomers for $n$=4 and $n$=6 cases were found, the other being a slightly altered gas-phase E structure. The symmetry of complexes in the continuous solvent was usually distorted and frequently the higher order $C_n$ group was no longer kept. Out of the three gas-phase isomers of $H^+(H_2O)_8$, only the (b) structure converged in the PCM calculations. The other two failed during the SCRF step, shortly after the optimization process had begun. Apart from the above-mentioned elongation of extremely short hydrogen bonds, a contraction of most of the hydrogen bonds in further hydration spheres occurred simultaneously, especially for more Eigen-like structures. The only comparable study has been provided by Tuñon *et al.*,[6] but their results in the continuum model have been obtained at the relatively low HF/6-31G* level. Unlike in the present work, they have concluded a lengthening of hydrogen bonds in the E-type $H_9O_4^+$ cation in the continuum with respect to the gas-phase. The decrease of the cluster volume observed by us seems, however, more probable, since such effect could in principle be expected due to the charge-continuum interaction.

The relative stabilities of studied PCM clusters were the

TABLE V. Average intermolecular oxygen-oxygen distances in different structural positions in the studied $H^+(H_2O)_n$ clusters at B3LYP/6-311++G($d$,$p$) level of theory and the corresponding vibrational frequencies.

| | | | Gas Phase | | PCM | |
|---|---|---|---|---|---|---|
| No. | Interpretation[a] | Distances[b] | $R_{OO}$[c] (Å) | $\nu^{o}_{OD}$[d] (cm$^{-1}$) | $R_{OO}$[c] (Å) | $\nu^{o}_{OD}$[d] (cm$^{-1}$) |
| I | Zundel 1° | 2-1; 4(a)-1;6 (a)-1; 8(c)-1 | 2.393 | 1535 | 2.420 | 1648 |
| II | Eigen 1° | 3-1,2; 4(b)-1,2,3; 5-1,2,3; 6(b)-1,2,4; 7-1,2,7;8.(a)-1,2,8; 8(b)-1,6,7 | 2.547 | 2056 | 2.534 | 2022 |
| III | Zundel 2° | 4(a)-2,3; 6(a)-2,3,4,5; 8(c)-2,3,4,5 | 2.653 | 2275 | 2.625 | 2224 |
| IV | Eigen 2° | 5-4; 6(b)-3,5; 7-3,5,6; 8(a)-3,5,7; 8(b)-5,8 | 2.698 | 2345 | 2.694 | 2339 |
| V | Zundel 3° | 8(c)-6,7 | 2.761 | 2424 | ⋯ | ⋯ |
| VI | Eigen 3° | 8(a)-6; 8(b)-4 | 2.749 | 2411 | 2.730 | 2388 |
| VII | "Donor pair"[e] | 7-4; 8(a)-4 | 2.878 | 2531 | 2.853 | 2512 |

[a]Consecutive hydration spheres denoted as 1°, 2°, 3°.
[b]The numbers, in the format of (cluster No.-bond No.), refer to respective labels in Fig. 7.
[c]Average of the distances from the "Distances" column.
[d]OD stretching band position calculated from the average distance (see text for details).
[e]See text for explanation.

same as for the gas-phase cases, but the energetic differences between isomeric forms were usually about two times greater.

### D. Experimental versus computational results: Proposed molecular model of hydration

The comparison of experimental and computational results might be achieved by comparing interatomic oxygen-oxygen distances, which can be obtained from the affected spectra. The numerical procedure and assumptions to the method have been previously discussed.[50] We used the $R_{OO}$ versus $\nu_{OD}$ correlation curve of Berglund *et al.*[48] Apart from the simple band position with distance correlation, our approach has also allowed calculation of distance probability distribution curves from absorption band shapes,[47,50] as proposed before.[42] The practical application of this method in the case of hydrated proton might be questioned, as the original correlation[48] does not reach below ca. 2000 $cm^{-1}$ and an anomal behavior of the relationship between stretching frequency and hydrogen bond length has been noted before.[68] Also, considerable dispersion of the $R_{OO}$ versus $\nu_{OH}$ correlation for HDO in liquid $D_2O$, primarily due to variations in the H-bond OHO angle, has been recently inferred from MD simulations.[69] Nevertheless, the results presented here for the aqueous proton clusters are in satisfactory agreement both with affected HDO spectra and with previous investigations for band positions above 2000 $cm^{-1}$.

In order to facilitate the comparison of theoretical and experimental vibrational frequencies, the *ab initio* obtained oxygen-oxygen distances were grouped into classes composed of bonds being in the same (or similar) geometric situation in different-sized clusters, separately for each level of theory. The details of the classification are outlined in Table V. The average distances, thus obtained, were next transformed into average OD band positions, using the above-mentioned correlation.[48] These may be compared with the experimental values gathered in Table I.

We did not apply analytically calculated vibrational frequencies for the comparison with affected HDO spectra, as we verified that they poorly correlated with experimental results for liquid water, even when scaled or otherwise corrected for anharmonicity. The geometry of the *ab initio* optimized clusters may be treated, on the other hand, as a snapshot picture of water affected by a solute and allowed us to recognize the perturbation introduced by the $H^+$ ion the bulk phase, observed in a very short time period, as in infrared spectroscopy. Averaging interatomic distances among differently sized clusters that we applied reflected the naturally broad distribution of possible geometric structures in liquid water. The optimization process, referring to molecular geometry at 0 K, naturally tended to shorten interatomic distances with respect to room temperature. The opposite effect resulted from the lack of H-bond cooperativity with the bulk phase, which normally shortens the intermolecular distances of interacting molecules. As a net effect, we observed shortening of $R_{OO}$ values obtained from calculated structures by ca. 0.02 Å relative to spectral data. According to the $R_{OO}$ versus $\nu_{OD}$ correlation curve,[48] this difference caused the redshift of frequencies derived from calculations—greater for low-wave-number component bands and very slight for high-wave-number part of the spectrum.

Based on Table V, we conclude that the central short and strong hydrogen bond in the Zundel cation was solely responsible for the most redshifted band in the affected spectrum. The $\nu^o_{OD}$ values found in the PCM calculations were much greater than their gas-phase counterparts, establishing a distorted, asymmetric Z structure in aqueous solutions, as predicted before by several authors.[13] The average PCM $\nu^o_{OD}$ became even further blueshifted if the shortest distance, taken from the $H_5O_2^+$ cluster, was excluded from the group. It then approached ca. 1700 $cm^{-1}$, which was also the average value of the component band position in the affected spectra (Table I). The agreement between experiment and computation in this part of the affected spectrum was debatable, as already discussed above.

The low-wave-number band was blueshifted with temperature (Fig. 4), indicating an increase of the length and asymmetry of the bond. On the synchronous correlation map the cross peaks appeared at ca. 1670 $cm^{-1}$ and were positively correlated with the 2530 $cm^{-1}$ band and negatively correlated with the 2672 and 2050 $cm^{-1}$ bands. Especially the latter effect seems significant, when we take into account that it most probably represents the first hydration sphere within E-type cation (see below). Negative correlation suggests that with temperature, the relative proportion of the Z-type cation to the E-type cation decreases.

The hydrogen bonds in the first coordination sphere of $H_3O^+$ Eigen cation were systematically longer than in the Zundel cation by ca. 0.11 Å (in the PCM approach). The average $\nu^o_{OD}$ derived from cluster structures was ca. 2050–2000 $cm^{-1}$, but the experimental affected spectra only contained a band some 50–100 $cm^{-1}$ below. Furthermore, the interpretation of this band as specific to hydrated proton is questionable (see Sec. IV A). As mentioned above, a cross peak at the correct wave number could be located on 2D correlation maps, however, indicating the presence of a regular Eigen cation, albeit at rather low concentration. Diffraction studies unanimously found a symmetrically hydrated proton as the preferred structure in concentrated acidic solutions.[70–72]

The second hydration sphere of a Z-type cation manifested itself in the affected spectra at ca. 2200 $cm^{-1}$, as suggested by Table I. No other distance group was located at this position and the PCM model results were very close to experimental ones, unlike gas-phase results. This further strengthens the proposition that an asymmetric Zundel cation might be the dominant structure in fairly diluted aqueous solutions. To visualize this effect and to help in inferring spectral and energetic characteristics of water H bonds, Fig. 8 can be proposed. It shows OD stretching band position related to asymmetry of hydrogen bond defined by[9,10]

$$q = \frac{R_{OO}}{2} - R_{OH}. \tag{2}$$

The presented correlation utilizes 6-311++G($d$,$p$) structures calculated in this work and already cited experimental data linking $\nu^o_{OD}$ with $R_{OO}$ and $R_{OH}$.[48] It is readily

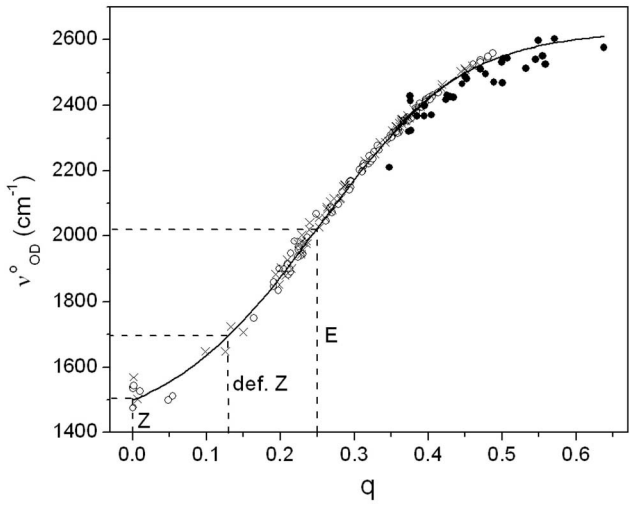


FIG. 8. Dependence of the HDO band position at maximum, $\nu^{o}_{OD}$, on the asymmetry of hydrogen bond, $q$, for the 6-311++G($d$,$p$) optimized gas-phase (open circles) and PCM-solvated (crosses) hydrated proton clusters and from the experimental neutron diffraction results for solid salt hydrates (solid circles) (Ref. 48). Dashed lines indicate ideal Zundel (Z) and Eigen (E) cations and the deformed Zundel cation (def. Z) detected in this work in the affected HDO spectra.

seen that the distances derived from pseudosymmetric $H^+(H_2O)_4$ and $H^+(H_2O)_6$ clusters in the PCM approximation form a separate group at $q \approx 0.13$ and $\nu^{o}_{OD} \approx 1700$ cm$^{-1}$. This value, transformed to interatomic distance, given $R_{OO} \approx 2.433$ Å, remarkably close to the *ab initio* MD results by Asthagiri *et al.*[13]

Distance groups IV, V, and VI (Table V) were all relatively close to each other. This suggests that further hydration spheres of Zundel and Eigen cations are similar and responsible for a single component in the affected spectrum. Groups V and VI are based on a small number of instances, due to limited size of the clusters. Nevertheless, the average distance was fairly preserved in various levels of theory. The "icelike" structure of water is thus the best description for third hydration sphere of the proton, in terms of average HDO band position.[62]

Distance group VII deserves special attention. Although based on only two bonds in two different size clusters, it was the only one with significantly longer distances. Both clusters adopted Z-type structure, with a "$H_3O^+ + H_2O$" complex. The geometric situation of discussed bond is meaningful: the donor electron pair is located on the $H_2O$ molecule from the central complex. It has been known from diffraction studies that one longer distance has been found in the hydrated proton complex.[71] Recent neutron diffraction study has concluded that the molecule in question is loosely bound with the central $H_3O^+$ ion. No hydrogen bond has been detected, but only weak orientational correlation at a distance greater than 2.8 Å.[70] The directional character of the hydrogen bond predicted in our calculations probably resulted from the small size of studied clusters. The experimental position of this band changed with temperature from 2546 cm$^{-1}$ at 10 °C to 2568 cm$^{-1}$ at 45 °C (Fig. 4), and on the correlation maps it appeared as a weak cross peak at 2562 cm$^{-1}$.

It might be further supposed that apart from the mentioned longer hydrogen bond in the immediate vicinity of hydrated proton, similar bonds exist in the hydration spheres beyond the icelike water, in parallel to the layered structure of hydration shells of metal cations.[45] Since the third hydration sphere is represented in the affected spectrum by the 2420 cm$^{-1}$ band, the next component would refer to the fourth hydration sphere. This was evidenced by appearance of numerous cross peaks at ca. 2530 cm$^{-1}$ in the 2D-IR spectrum. There are no computational data to support this, however, since that would require much larger clusters, beyond available machine resources.

## V. SUMMARY AND CONCLUSIONS

The structure of hydrated proton solvation shells, revealed by affected HDO spectra, seems very complex, but essentially follows the structure of hydrated metal cations. By combining experimental and computational results, we were able to discriminate several hydration shells around the central proton.

Computed cluster geometries and relative energies of isomeric clusters were fairly independent of the basis set, so 6-311++G($d$,$p$) basis proved to be sufficient for the present work. Reoptimization of the clusters in the continuous solvating medium, however, significantly affected the symmetry of complexes and therefore seemed necessary for deeper understanding of the structure of aqueous solutions. The agreement between experimental data and computations in the PCM approach was much greater than for gas-phase computed structures.

The dominant structure in fairly diluted aqueous solutions was identified as an asymmetric variant of the regular Zundel cation, intermediate between the ideal Z-type and E-type structures. Ample evidence was found for the existence of strong and short hydrogen bonds, with oxygen-oxygen distance about 2.42–2.44 Å in the PCM calculations on larger clusters, and only slightly longer when computed from the experimental affected spectra (maximum of 2.45 Å, average of 2.433 Å, at 25 °C). In conclusion, the excess proton appeared to form a "halfway" Zundel hydration complex, as predicted in the *ab initio* MD simulations.[13]

The ideal Eigen cation was poorly detectable in our experiment. The adequate component band was found only on 2D correlation maps prepared from temperature series. This contradicts the results of diffraction studies, but such experiments were conducted for rather concentrated solutions of acids.

Converged $H^+(H_2O)_n$ cluster structures allowed us to characterize further well-defined hydration spheres of excess proton. The second hydration sphere of Zundel cation manifested itself by a component band at ca. 2200 cm$^{-1}$ in the affected spectra, as accurately predicted by computed structures, especially in the PCM approach.

The third hydration sphere of Zundel cation and the second and third hydration spheres of Eigen cation were visible as a component band attributed previously to icelike water (at ca. 2420 cm$^{-1}$).

Fourth hydration sphere of the Zundel cation would

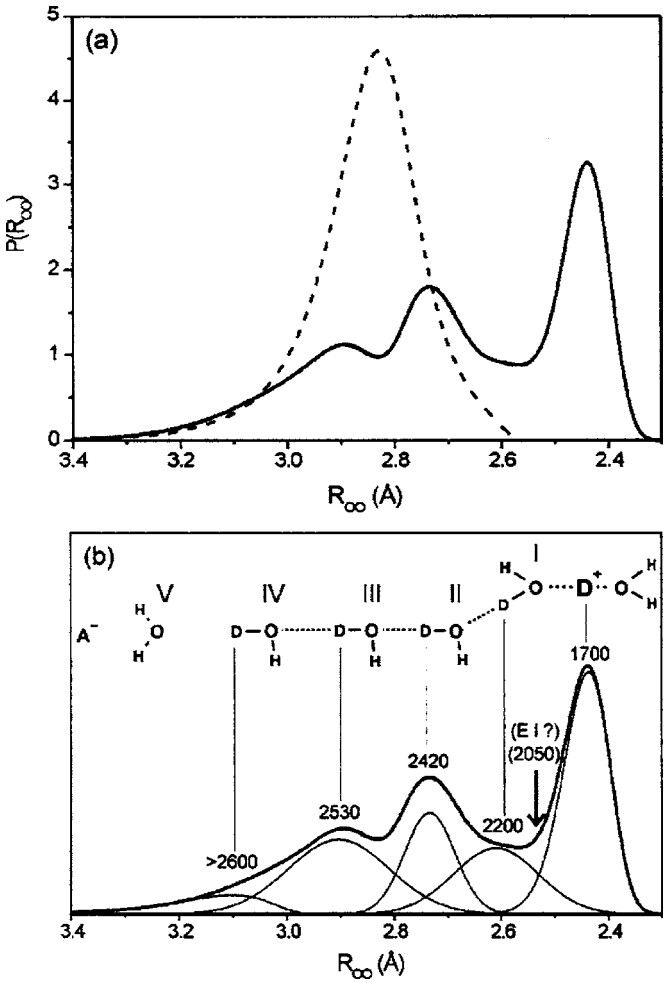


FIG. 9. (a) Interatomic oxygen-oxygen distance distribution derived from the spectrum of HDO affected by hydrated proton in $HPF_6$ aqueous solution at 298 K (solid line) along with bulk HDO distance distribution curve (dashed line). (b) Decomposition of the $P(R_{OO})$ curve for $HPF_6$ into contributions from consecutive hydration spheres (indicated by Roman numbers) of the deformed Zundel cation. Average component band positions in the HDO spectrum ($\nu_{OD}$,$cm^{-1}$) are shown above the curve for comparison and linked to corresponding OD oscillators. The expected distance and position for the first hydration sphere of regular Eigen cation (component detected only on the 2D IR correlation maps) are indicated by the arrow, the theoretically predicted distances in its second and third hydration spheres would contribute within the 2420 $cm^{-1}$ component.

manifest itself at the 2530 $cm^{-1}$ level, as predicted by the generalized model of cation hydration.[45] Limited size of the studied clusters did not allow direct comparison with experiment. In the light of the computational results, this band would be shared with the molecules interacting with the free electron pair of the central cation or an adjacent water molecule in its first hydration sphere.

Even further hydration spheres were visible in the affected spectra as shared "cation and anion-affected" water (above 2600 $cm^{-1}$), found previously for alkali metal cations.[47] The extent of deformation of Zundel cation depended on the anion. This influence was probably transmitted by the water molecules interacting with the free electron pairs of the central complex, which were affected by the anion. Their interactions with the complex depended also significantly on temperature.

All of the above observations might be confronted with the interatomic oxygen-oxygen distance distribution curve, shown in Fig. 9(a), calculated following the published procedure.[50] The curve, derived from the spectrum of HDO affected by $HPF_6$ at 298 K, after removal of component bands not attributed to the hydrated proton, displays a structure different than for any other ion in an aqueous solution. Figure 9(b) presents an illustrative diagram of the proposed hydration structure of the deformed Zundel cation, linking OD oscillator frequencies with respective contributions to the distance distribution curve. Expected position of the first hydration sphere of a regular Eigen cation is also indicated there and clearly the curve shows no marked structure in the immediate vicinity of this point.

Thus, the hydrated proton is a unique ion. It was evidenced for the first time that it possesses four well-defined hydration spheres, plus the outer hydration layer, shared with the anion. All spheres were characterized in terms of hydrogen bonds' lengths and arrangements. No other individuum displays such possibility to organize the structure of water: in the first three hydration spheres water is strongly ordered, in the following two water structure is broken.

## ACKNOWLEDGMENTS

Calculations in GAUSSIAN 03 were carried out at the Academic Computer Center in Gdańsk (TASK). Financial support from Center of Excellence in Environmental Analysis & Monitoring in Gdańsk (CEEAM) in the purchase of GAUSSIAN 03W and GAUSSVIEW 3.0 programs is acknowledged. Experimental work was supported by internal grants from Gdańsk University of Technology.

[1] R. P. Bell, *The Proton in Chemistry* (Cornell University Press, New York, 1959).
[2] G. A. Jeffrey and W. Saenger, *Hydrogen Bonding in Biological Structures* (Springer, Berlin, 1994).
[3] G. Zundel, in *The Hydrogen Bond: Recent Developments in Theory and Experiments*, edited by P. Schuster, G. Zundel, and C. Sandorfy (North-Holland, Amsterdam, 1976), Vol. II, p. 683.
[4] E. Wicke, M. Eigen, and T. Ackermann, Z. Phys. Chem., Neue Folge **1**, 340 (1954).
[5] N. Agmon, Chem. Phys. Lett. **244**, 456 (1995).
[6] I. Tuñon, E. Silla, and J. Bertran, J. Phys. Chem. **97**, 5547 (1993).
[7] A. Khan, Chem. Phys. Lett. **319**, 440 (2000).
[8] Y. Kim and Y. Kim, Chem. Phys. Lett. **362**, 419 (2002).
[9] D. Wei and D. R. Salahub, J. Chem. Phys. **101**, 7633 (1994).
[10] D. Wei and D. R. Salahub, J. Chem. Phys. **106**, 6086 (1997).
[11] G. Corongiu, R. Kelterbaum, and E. Kochanski, J. Phys. Chem. **99**, 8038 (1995).
[12] M. C. Vicens and G. E. Lopez, J. Comput. Chem. **21**, 63 (2000).
[13] D. Asthagiri, L. R. Pratt, and J. D. Kress, Proc. Natl. Acad. Sci. U.S.A. **102**, 6704 (2005).
[14] M. E. Tuckerman, K. Laasonen, M. Sprik, and M. Parrinello, J. Phys. Chem. **99**, 5749 (1995).
[15] J. Kim, U. W. Schmitt, J. A. Gruetzmacher, G. A. Voth, and N. E. Scherer, J. Chem. Phys. **116**, 737 (2002).
[16] U. W. Schmitt and G. A. Voth, J. Chem. Phys. **111**, 9361 (1999).
[17] U. W. Schmitt and G. A. Voth, Chem. Phys. Lett. **329**, 36 (2000).
[18] R. Vuilleumier and D. Borgis, J. Chem. Phys. **111**, 4251 (1999).
[19] H.-P. Cheng, J. Phys. Chem. A **102**, 6201 (1998).
[20] R. Kelterbaum and E. Kochanski, J. Phys. Chem. **99**, 12493 (1995).
[21] M. Cossi, V. Barone, R. Cammi, and J. Tomasi, Chem. Phys. Lett. **255**, 327 (1996).
[22] J. R. Pliego and J. M. Riveros, J. Phys. Chem. A **105**, 7241 (2001).
[23] R. E. Verrall, T. H. Lilley, B. E. Conway, and W. A. P. Luck, in *Water; A Comprehensive Treatise*, edited by F. Franks (Plenum, New York, 1973), Vol. 3.

[24] B. E. Conway, *Ionic Hydration in Chemistry and Biophysics* (Elsevier, Amsterdam, 1981), Chap. 7 and 8.
[25] C. I. Ratcliffe and D. E. Irish, Can. J. Chem. **62**, 1134 (1984).
[26] P. A. Giguere and J. G. Guillot, J. Phys. Chem. **86**, 3231 (1982).
[27] W. R. Busing and D. F. Hornig, J. Phys. Chem. **65**, 284 (1961).
[28] T. Ackermann, Z. Phys. Chem., Neue Folge **27**, 253 (1961).
[29] I. Kampschulte-Scheuing and G. Zundel, J. Phys. Chem. **74**, 2363 (1970).
[30] M. Leuchs and G. Zundel, J. Phys. Chem. **82**, 1632 (1978).
[31] M. Leuchs and G. Zundel, Can. J. Chem. **58**, 311 (1980).
[32] N. B. Librovich, V. P. Sakun, and N. D. Sokolov, Chem. Phys. **39**, 351 (1979).
[33] P. Rhine, D. Williams, G. M. Hale, and M. R. Querry, J. Phys. Chem. **78**, 1405 (1974).
[34] K. Zawada and P. Dryjański, J. Mol. Struct. **560**, 283 (2001).
[35] R. Janoschek, E. G. Weidemann, H. Pfeiffer, and G. Zundel, J. Am. Chem. Soc. **94**, 2387 (1972).
[36] P. A. Giguere, J. Chem. Educ. **56**, 571 (1979).
[37] J.-C. Jiang, Y.-S. Wang, H.-C. Chang, S. H. Lin, Y. T. Lee, G. Niedner-Schatteburg, and H.-C. Chang, J. Am. Chem. Soc. **122**, 1398 (2000).
[38] R. D. Waldron, J. Chem. Phys. **26**, 809 (1957).
[39] D. F. Horning, J. Chem. Phys. **40**, 3119 (1964).
[40] M. Falk and T. A. Ford, Can. J. Chem. **44**, 1699 (1966).
[41] O. Kristiansson, A. Eriksson, and J. Lindgren, Acta Chem. Scand., Ser. A **38**, 609 (1984).
[42] O. Kristiansson, A. Eriksson, and J. Lindgren, Acta Chem. Scand., Ser. A **38**, 613 (1984).
[43] O. Kristiansson, J. Lindgren, and J. de Villepin, J. Phys. Chem. **92**, 2680 (1988).
[44] J. Stangret, Spectrosc. Lett. **21**, 369 (1988).
[45] J. Stangret and T. Gampe, J. Phys. Chem. A **106**, 5393 (2002) and references therein.
[46] R. M. Badger and S. H. Bauer, J. Chem. Phys. **5**, 839 (1937).
[47] M. Śmiechowski, E. Gojlo, and J. Stangret, J. Phys. Chem. B **108**, 15938 (2004).
[48] B. Berglund, J. Lindgren, and J. Tegenfeldt, J. Mol. Struct. **43**, 169 (1978).
[49] H. D. Lutz and C. Jung, J. Mol. Struct. **404**, 63 (1997).
[50] J. Stangret and T. Gampe, J. Phys. Chem. B **103**, 3778 (1999).
[51] J. Stangret and E. Kamieńska-Piotrowicz, J. Chem. Soc., Faraday Trans. **93**, 3463 (1997).
[52] R. Krishnan, J. S. Binkley, R. Seeger, and J. A. Pople, J. Chem. Phys. **72**, 650 (1980).
[53] T. H. Dunning, J. Chem. Phys. **90**, 1007 (1989).
[54] R. Kendall, T. H. Dunning, and R. J. Harrison, J. Chem. Phys. **96**, 6796 (1992).
[55] C. Møller and M. S. Plesset, Phys. Rev. **46**, 618 (1934).
[56] A. D. Becke, J. Chem. Phys. **98**, 5648 (1993).
[57] A. D. Becke, Phys. Rev. A **38**, 3098 (1988).
[58] C. Lee, W. Yang, and R. G. Parr, Phys. Rev. B **37**, 785 (1993).
[59] H. B. Schlegel, J. Comput. Chem. **3**, 214 (1982).
[60] P. Csaszar and P. Pulay, J. Mol. Struct.: THEOCHEM **114**, 31 (1984).
[61] M. J. Frisch, G. W. Trucks, H. B. Schlegel *et al.*, GAUSSIAN 03, Revision B.05 and GAUSSIAN 03W, Revision C.02, Gaussian, Inc., Wallingford, CT, 2004.
[62] M. Falk, Can. J. Chem. **49**, 1137 (1971).
[63] W. A. P. Luck, in *Structure of Water and Aqueous Solutions*, edited by W. A. P. Luck (Chemie, Weinheim, 1974), p. 221.
[64] I. Noda, Appl. Spectrosc. **47**, 1329 (1993).
[65] N. E. Schultz, Y. Zhao, and D. G. Truhlar, J. Phys. Chem. A **109**, 11127 (2005).
[66] A. P. Scott and L. Radom, J. Phys. Chem. **100**, 16502 (1996).
[67] P. L. Fast, J. Corchado, M. L. Sanchez, and D. G. Truhlar, J. Phys. Chem. A **103**, 3139 (1999).
[68] A. Novak, Struct. Bonding (Berlin) **18**, 177 (1974).
[69] K. B. Møller, R. Rey, and J. T. Hynes, J. Phys. Chem. A **108**, 1275 (2004).
[70] A. Botti, F. Bruni, S. Imberti, M. A. Ricci, and A. K. Soper, J. Chem. Phys. **121**, 7840 (2004).
[71] R. Triolo and A. H. Narten, J. Chem. Phys. **63**, 3624 (1975).
[72] H.-G. Lee, Y. Matsumoto, T. Yamaguchi, and H. Ohtaki, Bull. Chem. Soc. Jpn. **56**, 443 (1983).